

Hot electron relaxation: Exact solution for a many electron model

K. Schönhammer and C. Wöhler

*Institut für Theoretische Physik der Universität Göttingen,
Bunsenstr.9, D-37073 Göttingen, Germany*

Abstract

The exact nonequilibrium time evolution of the momentum distribution for a finite many particle system in one dimension with a linear energy dispersion coupled to optical phonons is presented. For distinguishable particles the influence function of the phonon bath can be evaluated also for a finite particle density in the thermodynamic limit. In the case of fermions the exact fulfillment of the Pauli principle involves a sum over permutations of the electrons and the numerical evaluation is restricted to a finite number of electrons. In the dynamics the antisymmetry of the wavefunction shows up in the obvious Pauli blocking of momentum states as well as more subtle interference effects. The model shows the expected physical features known from approximate treatments of more realistic models for the relaxation in the energy regime far from the bottom of the conduction band and provides an excellent testing ground for quantum kinetic equations.

PACS numbers: 71.38.+i, 78.47.+p, 72.10.Bg

I. INTRODUCTION

The short time evolution of the relaxation of hot electrons due to the emission of optical phonons is not properly described using a Boltzmann equation, which assumes energy conserving independent scattering events, but requires the use of quantum kinetic equations [1–4]. Uncontrolled approximations involved in the derivation of these equations can lead to unphysical results such as negative probabilities for the momentum distribution. For the testing of new approximations it is very useful to find exactly solvable models, which show the main expected properties. We recently proposed two one-dimensional models for the relaxation of a *single* electron in which the energy dispersion of the excited electron is linearized around the initial energy high in the conduction band. In the first model [5] an infinite Fermi sea, as in the Tomonaga-Luttinger-model [6] is included. This can be viewed as a crude model for the relaxation in a doped semiconductor, while the second model without the Fermi sea [7] is more relevant for undoped semiconductors. *Exact* results for the momentum distribution were presented and compared with various improved quantum kinetic equations.

In a typical experimental situation a finite density of electrons is optically excited into the valence band. The nonequilibrium momentum distribution can be inferred from energy resolved measurements of transmission changes $\Delta T/T$ with delay times in the femtosecond range [10]. For their theoretical discussion of the results for GaAs these authors have compared approximate calculations in more realistic band structures with our second model [7] and “find the 1D linear model to be well justified as long as the carriers do not reach the bottom of the band”. For a more detailed study of the relaxation process it is necessary to treat the two effects properly which are not correctly described if the results of the single electron model are simply superposed according to the density of the excited electrons. A phonon emitted by one electron can be reabsorbed by another one leading to energy gain satellites in the momentum distribution. In the relaxation of many electrons the Pauli principle has to be taken into account. In a Boltzmann equation or typical quantum kinetic equations the

Pauli blocking of states is only treated in an *average* way and no exact description has been provided previously. In this paper we generalize our second model [7] to the *many* electron case and again obtain the exact solution for the nonequilibrium momentum distribution.

In Sec. II we present the model and its solution for two cases. We first assume the “electrons” to be distinguishable. Under this assumption the results for finite systems with a finite number of particles can be extended to the thermodynamic limit with a finite *density* of particles. The results show the importance of the gain processes mentioned earlier. If the fermionic character of the “electrons” is properly taken into account, the result for the momentum distribution contains a sum over permutations of $N - 1$ electrons and a numerical evaluation of the exact result is only possible for finite systems. For not too large electron-phonon coupling we also present an excellent approximation to the exact results which can be evaluated for larger systems. The model allows a detailed study in which parameter regimes a proper treatment of the Pauli blocking is of importance. Interference effects which are not correctly described by the usual quantum kinetic equations are shown to be especially important in the gain region. Some analytical and numerical details of the solution as well as a comparison with time dependent perturbation theory are presented in appendices.

II. THE MODEL AND ITS SOLUTION

In generalization of the polaron model presented in [7] we study a one-dimensional model of the relaxation of N “hot” particles due to the interaction with optical phonons. In order to obtain the exact solution of the time dependent Schrödinger equation we assume a *linear* energy dispersion for the particles. The Hamiltonian for a finite system of length L with periodic boundary conditions reads

$$H = H_e + H_p + H_{ep} = H_0 + H_{ep} \quad (1)$$

with

$$\begin{aligned}
H_e &= v \sum_{i=1}^N \hat{p}_i \quad , \quad H_p = \sum_q \omega_q b_q^\dagger b_q \quad , \\
H_{ep} &= \left(\frac{2\pi}{L} \right)^{1/2} \sum_q g(q) (\rho_q^\dagger b_q + b_q^\dagger \rho_q) \quad ,
\end{aligned} \tag{2}$$

where v is the velocity of the particles and b_q^\dagger the creation operator of a phonon with frequency ω_q . All the numerical results presented in Secs. III and IV are for optical phonons with a constant phonon frequency $\omega_q \equiv \omega_0$. The “electron-phonon” coupling strength given by $g(q)$ is specified later and the operator ρ_q denotes the Fourier transform of the particle density

$$\rho_q = \sum_{i=1}^N e^{-iq\hat{x}_i}. \tag{3}$$

We will discuss the case of distinguishable particles as well as the model with N spinless fermions. Due to the linear dispersion the model has no ground state. In the fermionic case this could be altered by adding an infinite Dirac sea. This is *not* considered in the following and we study the relaxation of an initial state with initial momenta k_1^0, \dots, k_N^0 and the phonons in their unperturbed ground state or in thermal equilibrium at a finite temperature. The exact description of the time dependence is possible due to the commutation relation $[\hat{x}_i, H] = iv\mathbb{1}$, which leads to

$$\rho_q(t) = e^{iHt} \rho_q e^{-iHt} = e^{-iqvt} \rho_q \tag{4}$$

independent of the coupling strength $g(q)$. The Heisenberg equation for $b_q(t)$ reads

$$i \frac{d}{dt} b_q(t) = \omega_q b_q(t) + \left(\frac{2\pi}{L} \right)^{1/2} g(q) \rho_q(t). \tag{5}$$

The solution of this inhomogeneous equation follows with (4)

$$b_q(t) = e^{-i\omega_q t} \left[b_q + \left(\frac{2\pi}{L} \right)^{1/2} g(q) \left(\frac{e^{-i(vq-\omega_q)t} - 1}{vq - \omega_q} \right) \rho_q \right] . \tag{6}$$

Therefore the change of the expectation value of the number of phonons $N_q = b_q^\dagger b_q$ due to the presence of the particles is determined by the expectation value of $\rho_q^\dagger \rho_q$ in the initial state

$$\delta \langle N_q \rangle (t) = \frac{2\pi}{L} |f_q(t)|^2 \langle \rho_q^\dagger \rho_q \rangle \quad (7)$$

with

$$|f_q(t)|^2 = g^2(q) \left(\frac{\sin [(\omega_q - vq) t/2]}{(\omega_q - vq)/2} \right)^2. \quad (8)$$

This will be discussed in Secs. III and IV. We first present the method to calculate expectation values of an operator A acting in the Hilbert space of the particles, i. e. $A = |k\rangle_{(i)} \langle k|$, where $A = |k\rangle_{(i)}$ is the momentum state in the Hilbert space of the particle i . For the case of indistinguishable particles we will consider one-particle operators $A = \sum_{i=1}^N A_{(i)}$. We present the result for expectation values $\langle A \rangle (t)$ for a statistical operator of the initial state which factorizes into a particle and a phonon part, i. e. $\rho_0 = \rho_p \cdot \rho_{ph}$. We work in the interaction representation and denote the time evolution with the unperturbed Hamiltonian by $A_D(t)$. Due to the simple form of $\rho_{q,D}(t) = e^{-iqvt} \rho_q$ it is favorable to perform the trace in the particle Hilbert space using the position states $|\mathbf{x}\rangle \equiv |x_1\rangle_1 \otimes \cdots \otimes |x_N\rangle_N$. This yields

$$\langle A \rangle (t) = \int d\mathbf{x}' d\mathbf{x} \langle \mathbf{x}' | \rho_p | \mathbf{x} \rangle Tr_{ph} \left[\rho_{ph} \langle \mathbf{x} | \tilde{U}^\dagger(t) A_D(t) \tilde{U}(t) | \mathbf{x}' \rangle \right], \quad (9)$$

where $\tilde{U}(t) \equiv e^{iH_0 t} e^{-iHt}$ is the time evolution operator in the interaction representation. The proper projection on the totally antisymmetric states in the case of fermions is taken care of by the statistical operator ρ_p . In the following we assume ρ_p to describe a *translational invariant* initial state, i. e. ρ_p is diagonal in the momentum representation. The simple form of $\rho_{q,D}(t)$ implies that the only electronic operators in $H_{ep,D}(t)$ are the commuting position operators \hat{x}_i . Therefore $\tilde{U}(t) |\mathbf{x}'\rangle = \tilde{U}_{\mathbf{x}'}(t) |\mathbf{x}'\rangle$, where $\tilde{U}_{\mathbf{x}'}(t)$ is an operator in the *phonon* Hilbert space only. This allows us to write Eq.(9) in the form

$$\langle A \rangle (t) = \int d\mathbf{x}' d\mathbf{x} \langle \mathbf{x}' | \rho_p | \mathbf{x} \rangle \langle \mathbf{x} | A_D(t) | \mathbf{x}' \rangle F(\mathbf{x}, \mathbf{x}', t), \quad (10)$$

where the “influence function” $F(\mathbf{x}, \mathbf{x}', t)$ is given by

$$F(\mathbf{x}, \mathbf{x}', t) = Tr_{ph} \left[\rho_{ph} \tilde{U}_{\mathbf{x}}^\dagger(t) \tilde{U}_{\mathbf{x}'}(t) \right]. \quad (11)$$

The differential equation for $\tilde{U}_{\mathbf{x}}(t)$ reads

$$i \frac{d}{dt} \tilde{U}_{\mathbf{x}}(t) = \left(C_{\mathbf{x}}(t) + C_{\mathbf{x}}^\dagger(t) \right) \tilde{U}_{\mathbf{x}}(t) \quad (12)$$

with

$$C_{\mathbf{x}}(t) = \left(\frac{2\pi}{L} \right)^{1/2} \sum_q g(q) e^{-i(\omega_q - vq)t} \rho_q^\dagger(\mathbf{x}) b_q \quad (13)$$

where $\rho_q(\mathbf{x})$ is the eigenvalue of the operator ρ_q in the state $|\mathbf{x}\rangle$. Using the Baker-Hausdorff formula the solution of equation (12) is straightforward [7]

$$\tilde{U}_{\mathbf{x}}(t) = \exp \left\{ -i \int_0^t C_{\mathbf{x}}^\dagger(t') dt' \right\} \exp \left\{ -i \int_0^t C_{\mathbf{x}}(t') dt' \right\} a_{\mathbf{x}}(t) \quad , \quad (14)$$

where $a_{\mathbf{x}}(t)$ is given by the *c*-number

$$a_{\mathbf{x}}(t) = \exp \left\{ -\frac{2\pi}{L} \sum_q \gamma_q(t) |\rho_q(\mathbf{x})|^2 \right\} \quad (15)$$

with

$$\gamma_q(t) = \frac{g^2(q)}{(\omega_q - vq)^2} \left(1 - i(\omega_q - vq)t - e^{-i(\omega_q - vq)t} \right) \quad . \quad (16)$$

The trace over the Hilbert space in Eq.(11) can be performed if the phonons are initially assumed to be in thermal equilibrium at temperature T . Then we can use $\langle e^A e^B \rangle = e^{\frac{1}{2} \langle A^2 + 2AB + B^2 \rangle}$, valid for canonical expectation values for free bosons and operators A and B *linear* in the boson creation and annihilation operators [8]. Using Eqs.(13) and (14) one obtains

$$F(\mathbf{x}, \mathbf{x}', t) = \exp \left\{ \frac{2\pi}{L} \sum_q |f_q(t)|^2 \left[\rho_q^*(\mathbf{x}) \rho_q(\mathbf{x}') - n_B(\omega_q) |\rho_q(\mathbf{x}) - \rho_q(\mathbf{x}')|^2 \right] \right\} a_{\mathbf{x}}^*(t) a_{\mathbf{x}'}(t), \quad (17)$$

where $n_B(\omega_q) = 1/(\exp(\omega_q/k_B T_{ph}) - 1)$ is the Bose function. With this analytical expression for the influence function the evaluation of expectation values of particle operators is reduced to integrations in Eq.(10).

We now specialize the operator \hat{A} to the momentum distribution and begin with distinguishable particles. For the operator $n_k^{(1)} \equiv |k\rangle_{(1)} \langle k|$ the integral in (10) simplifies as

$$\langle \mathbf{x} | n_k^{(1)} | \mathbf{x}' \rangle = \frac{1}{L} e^{ik(x_1 - x'_1)} \delta(\underline{\mathbf{x}} - \underline{\mathbf{x}}') \quad (18)$$

contains a delta function in the variables $\underline{\mathbf{x}} = (x_2, \dots, n_N)$ and $\underline{\mathbf{x}}'$. Therefore the influence function F is needed only for $\underline{\mathbf{x}}' = \underline{\mathbf{x}}$. In the variables $\tilde{x}_i \equiv x_i - x'_1$ one has

$$\rho_q^*(x_1, \underline{\mathbf{x}}) \rho_q(x'_1, \underline{\mathbf{x}}) = e^{iq\tilde{x}_1} + \sum_{j=2}^N (e^{iq(\tilde{x}_1 - \tilde{x}_j)} + e^{iq\tilde{x}_j}) + \sum_{i,j=2}^N e^{iq(\tilde{x}_i - \tilde{x}_j)} \quad (19)$$

and corresponding expressions for $|\rho_q(x_1, \underline{\mathbf{x}})|^2$ and $|\rho_q(x'_1, \underline{\mathbf{x}})|^2$. Due to the identity $\gamma_q^*(t) + \gamma_q(t) = |f_q(t)|^2$ the terms with the double sum involving two “other” particles cancel. This leads to

$$F(x_1, \underline{\mathbf{x}}; x'_1, \underline{\mathbf{x}}, t) = F_1(\tilde{x}_1, t) \prod_{i=2}^N \exp \left\{ \frac{2\pi}{L} \sum_q [\gamma_q^*(t) (e^{iq\tilde{x}_1} - 1) e^{-iq\tilde{x}_i} - \gamma_q(t) (e^{-iq\tilde{x}_1} - 1) e^{iq\tilde{x}_i}] \right\} \quad (20)$$

where

$$F_1(x, t) = \exp \left\{ \frac{2\pi}{L} \sum_q |f_q(t)|^2 \left[(e^{iqx} - 1) (1 + n_B(\omega_q)) + (e^{-iqx} - 1) n_B(\omega_q) \right] \right\} \quad (21)$$

is the influence function of a *single* particle [7].

Now the integration in Eq.(10) can be partially carried out using Eqs.(18) and (20) and one obtains

$$\langle n_k^{(1)} \rangle (t) = \int dx e^{ikx} \rho^{(1)}(x) F_1(x, t) (G_0(x, t))^{N-1} \quad (22)$$

with

$$G_0(x, t) = \frac{1}{L} \int dy \exp \left\{ \frac{2\pi}{L} \sum_q [\gamma_q^*(t) (e^{iqx} - 1) e^{-iqy} - \gamma_q(t) (e^{-iqx} - 1) e^{iqy}] \right\} \quad (23)$$

and $\rho^{(1)}(x)$ is given by the real space matrix elements of the reduced statistical operator for particle one for which the trace (tr') over the other particles has been performed

$$\rho^{(1)}(x_1 - x'_1) = L^{N-1} \langle x_1, \underline{\mathbf{x}} | \rho_p | x'_1, \underline{\mathbf{x}} \rangle = \langle x_1 | tr'(\rho_p) | x'_1 \rangle. \quad (24)$$

For $N = 1$ and $\rho^{(1)} = |k_1^0\rangle \langle k_1^0|$, i. e. $\rho^{(1)}(x) = \frac{1}{L} e^{-ik_1^0 x}$ Eq.(22) reduces to the polaron result presented in [7]. The result for $\langle n_k^{(1)} \rangle (t)$ will be analyzed in the next section.

We now turn to the case of N fermions. In first quantization the momentum occupation number operator \hat{n}_k reads in the Hilbert space $H_N^{(a)}$, where (a) denotes the subspace of antisymmetrized states

$$\hat{n}_k = \frac{1}{(N-1)!} \sum_{k_2, \dots, k_N} |k, k_2, \dots, k_N\rangle_{aa} \langle k_N, \dots, k_2, k| \quad (25)$$

The factor $1/(N-1)!$ is necessary because the $N-1$ summations are unrestricted. To calculate $\langle \hat{n}_k \rangle (t)$ we can proceed as in Eqs.(9) and (10) using product states $|\mathbf{x}\rangle$ which are *not* antisymmetrized. In the following we describe the time evolution of an initial state $|\mathbf{k}_0\rangle_a$. The result for an arbitrary translational invariant statistical operator is obtained by averaging the result with the normalized probability density $p(\mathbf{k}_0)$ describing ρ_p . The initial state $|k_1^0, \dots, k_N^0\rangle_a$ and the projectors in Eq.(25) take care of the Pauli principle. Using $\langle \mathbf{x} | \mathbf{k} \rangle_a = {}_a \langle \mathbf{x} | \mathbf{k} \rangle$ we obtain

$$\langle \mathbf{x} | \hat{n}_k | \mathbf{x}' \rangle = \frac{1}{L} \frac{1}{N!(N-1)!} \left[e^{ik(x_1-x'_1)} \delta(\underline{\mathbf{x}} - \underline{\mathbf{x}'}) \pm \dots \right], \quad (26)$$

where the parenthesis contains all $(N!)^2$ terms which result from antisymmetrizing the first term with respect to the \mathbf{x} *and* the \mathbf{x}' variables. As in Eq.(10) this expression is multiplied by the function $f(\mathbf{x}, \mathbf{x}', t) = \langle \mathbf{k}^0 | \mathbf{x} \rangle_a {}_a \langle \mathbf{x}' | \mathbf{k}^0 \rangle F(\mathbf{x}, \mathbf{x}', t)$, which is also antisymmetric in both the \mathbf{x} and \mathbf{x}' variables, the \mathbf{x} - and \mathbf{x}' - integrations yield $(N!)^2$ identical terms, i.e. one can just take the first term on the rhs of Eq.(26) and multiply it by $(N!)^2$

$$\langle \hat{n}_k \rangle = \frac{N}{L} \int dx_1 dx'_1 d\underline{\mathbf{x}} e^{ik(x_1-x'_1)} {}_a \langle \mathbf{k}^0 | x_1, \underline{\mathbf{x}} \rangle {}_a \langle x'_1, \underline{\mathbf{x}} | \mathbf{k}^0 \rangle_a F(x_1, \underline{\mathbf{x}}; x'_1, \underline{\mathbf{x}}, t). \quad (27)$$

Note that again only the special form of the arguments of the influence function as in Eq.(17) appear. Due to the translational invariance discussed there, the x'_1 -integration can be carried out by setting $x'_1 = 0$ in the remaining integrand and dropping the factor $1/L$. The factors in the integrand which take care of the Pauli principle can be written as

$${}_a \langle \mathbf{k}_0 | x_1, \underline{\mathbf{x}} \rangle {}_a \langle 0, \underline{\mathbf{x}} | \mathbf{k}_0 \rangle_a = \frac{1}{NL} \sum_{i,j=1}^N e^{ik_i^0 x_1} {}_a \langle \mathbf{k}^0 | c_{k_i^0}^\dagger | \underline{\mathbf{x}} \rangle {}_a \langle \underline{\mathbf{x}} | c_{k_j^0} | \mathbf{k}^0 \rangle_a \quad (28)$$

where the $c_k^\dagger (c_k)$ are the usual creation (annihilation) operators and the factor $1/N$ appears because we have switched from antisymmetrized N -particles states to antisymmetrized

$(N-1)$ -particle states. In Eq.(27) the rhs of Eq.(28) is integrated with a function *symmetric* in the $\underline{\mathbf{x}}$ variables. In writing out the factors ${}_a \langle \mathbf{k}^0 | c_{k_i^0} | \underline{\mathbf{x}} \rangle$ and $\langle \underline{\mathbf{x}} | c_{k_j^0} | \mathbf{k}^0 \rangle_a$ as antisymmetrical sums of $(N-1)!$ terms each term of the second sum yields the same contribution. Therefore for the use of the integration with a symmetric function in $\underline{\mathbf{x}}$ we can write

$${}_a \langle \mathbf{k}_0 | x_1, \underline{\mathbf{x}} \rangle \langle 0, \underline{\mathbf{x}} | \mathbf{k}_0 \rangle_a = \frac{1}{NL^N} \sum_{i,j=1}^N e^{i(k-k_i^0)x_1} \sum_{P_{N-1}} (-1)^{i+j+P_{N-1}} e^{-i \sum_{l=2}^N (k_{P_{N-1},l}^{0|i} - k_l^{0|j})x_l}. \quad (29)$$

Here we have introduced the notation ($l = 2, \dots, N$)

$$k_l^{0|j} \equiv \begin{cases} k_{l-1}^0 & (l \leq j) \\ k_l^0 & (l > j) \end{cases} \quad (30)$$

i.e. the upper index indicates the missing initial momentum. If one inserts (29) on the rhs of Eq.(27) one obtains

$$\langle n_k \rangle (t) = \sum_{i=1}^N \frac{1}{L} \int dx e^{i(k-k_i^0)x} F_1(x, t) G_{N-1}^{(i)}(x, t) \quad (31)$$

with

$$G_{N-1}^{(i)}(x, t) = \sum_{j=1}^N \sum_{P_{N-1}} (-1)^{i+j+P_{N-1}} \prod_{l=2}^N G(k_l^{0|j} - k_{P_{N-1},l}^{0|i}, x, t) \quad (32)$$

and

$$G(k, x, t) \equiv \frac{1}{L} \int dy e^{iky} \exp \left\{ \frac{2\pi}{L} \sum_q \left[\gamma_q^*(t) (e^{iqx} - 1) e^{-iqy} - \gamma_q(t) (e^{-iqx} - 1) e^{iqy} \right] \right\}. \quad (33)$$

This is a central result of our paper. The result for $\langle n_k \rangle (t)$ in Eq.(31) should be compared with the result for $\langle n_k^{(i)} \rangle (t)$ in Eq.(22) summed over all N particles. If all the initial momenta are different also for the distinguishable particles the total momentum distribution is given by Eq.(31) with $G_{N-1}^{(i)}(x, t)$ replaced by $(G_0(x, t))^{N-1}$. For fermions the sum over permutations in Eq.(32) is necessary in order to obey the Pauli principle exactly. While for distinguishable particles it is possible to obtain results for a finite *density* of particles in the thermodynamic limit as discussed in Sec.III, the more complicated expression for $G_{N-1}^{(i)}(x, t)$ can only be evaluated for a finite number of particles. The results are presented in Sec. IV.

III. RESULTS FOR DISTINGUISHABLE PARTICLES

As we are mainly interested in modelling aspects of hot electron relaxation in semiconductors, the fermion result Eq.(31) for the time dependence of the momentum occupation numbers is considered more important than the expression Eq.(22) for distinguishable particles. Due to the relative simplicity of the latter result compared to the fermionic one, it is useful to discuss Eq.(22) in order to obtain a first understanding of the difference between the cases $N = 1$ and $N > 1$.

The modification of the energy transfer to the phonons is trivial, as $\langle \mathbf{k}_0 | \rho_q^\dagger \rho_q | \mathbf{k}_0 \rangle = N$ for $q \neq 0$, i. e. the $N = 1$ polaron result is just multiplied by N in Eq.(7). In contrast to this simple expression, the occupancy $\langle n_k^{(1)} \rangle(t)$ for $N > 1$ differs *qualitatively* from the $N = 1$ result. With the phonons initially in their ground state *no* energy gain is possible for one particle, if in our model the q -sum in H in Eq.(1) is restricted to positive values. If the sum also includes negative q -values a small weight in the gain region occurs for short times but *no* resonant gain peak appears. In the following we therefore use two special choices for the coupling function of the “electron”-phonon interaction, $g^{(1)}(q) = g\Theta(q)\Theta(q_c - q)$, where q_c is a cutoff and $g^2(q) \equiv g$ for all $q \in (-\infty, \infty)$. As discussed in appendix A the latter choice allows the analytical calculation of the integrals in the influence function $F(\mathbf{x}, \mathbf{x}', t)$ in Eq.(17) in the thermodynamic limit. We start our discussion with the special case $\rho^{(1)} = tr' \rho_p = |k_1^0\rangle \langle k_1^0|$, i.e. particle one is initially in the state $|k_1^0\rangle$.

A straightforward perturbation expansion of $G_0(x)$ in Eq.(23) in powers of $\gamma \sim g^2$ shows that energy gain *is* possible for $N > 1$ in contrast to the $N = 1$ result for $g^{(1)}(q)$:

$$G_0(x, t) = 1 - \left(\frac{2\pi}{L}\right)^2 \sum_q \left\{ \left[|\gamma_q(t)|^2 + \text{Re}(\gamma_q(t)\gamma_{-q}(t)) \right] \left(2 - e^{iqx} - e^{-iqx} \right) \right\} + O(\gamma^3) \quad (34)$$

For the model with $g^{(1)}(q)$ the contribution proportional to e^{-iqx} leads to a nonzero weight in $\langle n_k^{(1)} \rangle(t)$ for $k > k_1^0$, i.e. energy gain. Only the term proportional to $|\gamma_q(t)|^2$ is nonzero and the probability for the gain process agrees with the result from squaring the amplitude in second order time dependent perturbation theory for the process in which

particle 2 emits a phonon, which is reabsorbed by particle 1 (see appendix C). As $|\gamma_q(t)|^2$ is of the order $(1/L)^0$ the probability of such a gain process goes to zero as $1/L$ for $L \rightarrow \infty$, if only two (or a finite number of) particles are present. It is therefore more interesting to study the thermodynamic limit for a finite (other) particle density $n_p \equiv (N-1)/L$. In the limit $L \rightarrow \infty$ the momentum distribution goes over to a function defined on \mathbb{R} . In order to normalize this function to one, $\langle n_k^{(1)} \rangle(t)$ has to be multiplied by the density of k-points, i. e. we consider the function $n(k, t) \equiv \lim_{L \rightarrow \infty} \left(\frac{L}{2\pi}\right) \langle n_k^{(1)} \rangle(t)$. As the function $G_0(x, t)$ in Eq.(23) has the form

$$G_0(x, t) = 1 + \frac{1}{N-1} n_p c_L(x, t), \quad (35)$$

where $c_L(x, t)$ goes over to a well defined limiting function $c(x, t)$ for $L \rightarrow \infty$, the factor $(G_0(x, t))^{N-1}$ in Eq.(22) has the $N \rightarrow \infty$ limit $\exp(n_p c(x, t))$. This yields with the normalized probability $p(k_1)$ for the initial momentum the exact finite density momentum distribution in the thermodynamic limit

$$n(k, t) = \int_{-\infty}^{\infty} dk_1 p(k_1) \int_{-\infty}^{\infty} \frac{dx}{2\pi} e^{i(k-k_1)x} e^{b(x, t) + n_p c(x, t)} \quad (36)$$

with

$$b(x, t) = \int_{-\infty}^{\infty} dq |f_q(t)|^2 \left[(e^{iqx} - 1) (1 + n_B(\omega_q)) + (e^{-iqx} - 1) n_B(\omega_q) \right] \quad (37)$$

and

$$c(x, t) = \int_{-\infty}^{\infty} dy \left[\exp \left\{ \int_{-\infty}^{\infty} dq \left[\gamma_q^*(t) (e^{iqx} - 1) e^{-iqy} - \gamma_q(t) (e^{-iqx} - 1) e^{iqy} \right] \right\} - 1 \right] \quad (38)$$

The function $c(x, t)$ cannot be determined completely analytically even for the coupling function $g^{(2)}(q) \equiv g$, as discussed in appendix A. It is therefore useful also to consider $c(x, t)$ in leading order perturbation theory in γ . Using Eq.(34) or (38) one obtains

$$c_2(x, t) = -2\pi \int_{-\infty}^{\infty} dq \left[|\gamma_q(t)|^2 + \text{Re}(\gamma_q(t)\gamma_{-q}(t)) \right] (2 - e^{iqx} - e^{-iqx}). \quad (39)$$

In this approximation the result for $n^{(1)}(k, t)$ has the same form as for a *single* particle and the phonons at finite temperature [7], but with the Bose function in Eq.(37) replaced by the

sum of $n_B(\omega_q)$ and the time dependent quantity $2\pi n_p \left[|\gamma_q(t)|^2 + \text{Re}(\gamma_q(t)\gamma_{-q}(t)) \right] / |f_q(t)|^2$. In order to estimate in which parameter range Eq.(39) provides a good approximation it is useful to introduce the dimensionless coupling constant $\alpha \equiv 2\pi g^2/(v\omega_0)$ and to multiply n_q by the relevant length $v/\omega_0 \equiv 1/q_B$ in our model. If in addition we introduce dimensionless time and space variables $\tau \equiv \omega_0 t$ and $u \equiv q_B x$, the finite density contribution $n_p c(x, t)$ in the exponent in Eq.(36) can be written as $(n_p/q_B) \tilde{c}(u, \tau)$ where \tilde{c} is a dimensionless function. The small density regime is given by $\tilde{n}_p \equiv n_p/q_B \ll 1$. For finite systems this corresponds to $(N - 1)/(2\pi n_B) \ll 1$, where n_B is the number of momentum states in an arbitrary momentum interval $(q, q + q_B)$. The use of $c^{(2)}(x, t)$ in Eq.(36) is certainly allowed in the low-density and small α regime.

For the special case of a sharp initial momentum $p(k_1) = \delta(k_1 - k_1^0)$ the momentum distribution $n(k, t)$ in Eq.(36) consists of a delta peak at $k = k_1^0$ with a weight $p_{k_1^0}(t) = \exp(b(\infty, t) + n_p c(\infty, t))$ and a continuous part which for finite times is nonzero for k_1^0 also. In Fig.1 we compare the time evolution of the weight $p_{k_1^0}(t)$ for the two different values of the dimensionless density $\tilde{n}_p = 10^{-3}$ and $\tilde{n}_p = 10^{-2}$ with the $N = 1$ polaron result. The dimensionless coupling constant has the small value $\alpha = 2\pi 10^{-3}$. The result for the coupling functions $g^{(1)}$ and $g^{(2)}$ do not differ on the scale of the figure. Obviously the presence of the other particles accelerates the relaxation process. In order to obtain a simple quantitative estimate of this effect we compare the exact result with the approximation to replace $c(\infty, t)$ by $c_2(\infty, t)$, where $c_2(\infty, t)$ is obtained by dropping the x -dependent part on the rhs of Eq.(39). In this approximation the exponential decay of the polaron case is replaced by the faster decay approximately given by $p_{k_1^0}(\tau) \approx \exp(-\alpha\tau - \frac{2}{3}\alpha^2\tilde{n}_p\tau^3)$, where we have used Eq.(A10). For dimensionless times τ larger than $(\alpha\tilde{n}_p)^{-1/2}$ the deviation from the polaron result becomes important.

In Fig.2 the first two curves represent the *continuous* part of the momentum distribution as a function of the dimensionless momentum variable $\tilde{k} \equiv k/q_B$ for $k_1^0 = 0$ and the weight of the delta peak is given in the figure captions. We compare the results for the coupling

functions $g^{(1)}$ and $g^{(2)}$ for the same values of the coupling α as in Fig.1 and $\tilde{n}_p = 10^{-3}$ at the time $\tau = 50$ where the influence of the other particles in the energy loss regime at negative momenta is still rather small. The momentum distribution shows loss features around $\tilde{k} = -1, -2$ and -3 corresponding to the emission of one, two and three phonons. The short time energy uncertainty well known from standard derivations of Fermi's golden rule is clearly visible, especially at the tails of the one phonon loss peak. For longer times these oscillations weaken and the peaks become narrower at the resonant positions. A rather small energy gain peak at $\tilde{k} = 1$ is also visible in Fig.2. A qualitative difference of the coupling functions $g^{(1)}$ and $g^{(2)}$ shows up at positive momenta. While the weight is strictly zero for $\tilde{n}_p = 0$ in this range for $g^{(1)}(q)$, the coupling $g^{(2)}(q)$ shows a weak oscillatory weight there as in the polaron case which survives in Fig.2. Within the plotting accuracy the results in this figure agree with the exact results, when $c(x, t)$ is approximated by $c_2(x, t)$ (Eq.(39)). For much larger times many sharp phonon replicas develop and the oscillations in the tails become weak. The difference between the $g^{(1)}$ and $g^{(2)}$ results become very small and the replacement of $c(x, t)$ by $c_2(x, t)$ is quantitatively no longer sufficient especially in the gain region. The oscillatory behaviour of both systems is smeared out and the peaks are broadened if a Gaussian probability distribution $p(k_1)$ is used in Eq.(36).

In Fig.3 the momentum distribution functions for the thermodynamic limit with different particle densities and for a finite system are compared at the time $\omega_0 t = 30$. Our method to perform the integration in Eq.(22) for finite systems is described in appendix B. Only the zero momentum state was initially excited but due to the larger coupling $\alpha = 2\pi 10^{-2}$ the curves are smoother and the relaxation faster. Also, for the first two systems with the larger particle density the energy uncertainty oscillations of the first resonant state are smeared out. They have the same dimensionless particle density, i.e. for the thermodynamic limit it is $n_p/q_B = 0.2/(2\pi)$ and the finite systems $n_p/q_B = (N - 1)/(2\pi n_B)$ where $q_B = \frac{2\pi}{L} n_B$. As can be seen the result for the finite system with nine particles is already very close to the result for the thermodynamic limit. At earlier times the two curves agree very well but then

the differences appear and grow with time advancing. For a smaller coupling this behaviour is slowed down, e. g. for $\alpha = 2\pi 10^{-3}$ the agreement is still excellent at time $\omega_0 t = 50$.

Comparing the first and the last system one can see that the gain satellites at positive momentum and also at momentum less than $-4q_B$ are much more pronounced for the larger density. Generally, a larger density smoothes the curves and accelerates the spreading of the peaks.

IV. RESULTS FOR FERMIONS

The role of the Pauli principle for more than one fermion is quite easily seen for the number of phonons created Eq.(7), while the momentum distribution Eq.(31) requires a much larger numerical effort than in the case of distinguishable particles.

In order to obtain $\delta \langle N_q \rangle (t)$ we have to evaluate the expectation value of $\rho_q^\dagger \rho_q$ in the fermionic initial state, which was taken as the Slater determinant $|\mathbf{k}^0\rangle_a$ in Sec. II. The expectation value can either be calculated using Wick's theorem using the method of second quantization or using first quantization as in Sec. II. For $q \neq 0$ one obtains

$$\begin{aligned} \langle \rho_q^\dagger \rho_q \rangle_{t=0} &= \sum_k \langle n_{k+q} \rangle (t=0) (1 - \langle n_k \rangle (t=0)) \\ &= N - \sum_{i,j=1}^N \delta_{k_i^0, k_j^0 + q}, \end{aligned} \quad (40)$$

where the first equality holds for an arbitrary initial Slater determinant. The second equality shows that the Pauli blocking on the energy transfer to the phonons is most prominent in the artificial state in which all the initial momenta are separated by q_B . Then $\langle \rho_{q_B}^\dagger \rho_{q_B} \rangle = 1$ and due to the Pauli blocking the number of phonons corresponding to the energy conserving transitions is reduced drastically compared to the case of distinguishable particles.

In order to calculate the momentum distribution Eq.(31) the functions $G_{N-1}^{(i)}$ have to be evaluated, which involve products of the functions $G(k, x, t)$ for different values of the momentum argument. We first discuss the behaviour of $G(k, x, t)$ in leading order perturbation

theory in the electron-phonon coupling g . Expanding the exponential function in Eq.(33) we obtain

$$\begin{aligned}
G(k, x, t) = & \delta_{k,0} + \left(\frac{2\pi}{L}\right) (\gamma_k^*(t) - \gamma_{-k}(t)) (e^{ikx} - 1) \\
& - \left(\frac{2\pi}{L}\right)^2 \sum_q \left[\gamma_{k+q}^*(t) \gamma_q(t) (1 + e^{ikx} - e^{i(k+q)x} - e^{-iqx}) \right. \\
& + \gamma_q^*(t) \gamma_{k-q}^*(t) (1 + e^{ikx} - e^{i(k-q)x} - e^{iqx}) / 2 \\
& \left. + \gamma_q(t) \gamma_{-k-q}(t) (1 + e^{ikx} - e^{i(k+q)x} - e^{-iqx}) / 2 \right] \\
& + O(\gamma^3).
\end{aligned} \tag{41}$$

In the sum over j on the rhs of Eq.(32) the term $i = j$ and the terms $j \neq i$ behave differently concerning a perturbation expansion. We first discuss the diagonal term. In the sum over the permutations the identity presents the leading approximation given by $(G_0(x, t))^{N-1}$, i.e. this contribution to $G_{N-1}^{(i)}(x, t)$ is identical to the exact result for distinguishable particles. The contributions of the other permutations are of the order $(\gamma/L)^m G_0^{N-1-m}$ with $m \geq 2$. For $i \neq j$ there is no term in which all momentum differences vanish. The leading term in γ/L is given by $-G(k_i^0 - k_j^0, x, t)(G_0(x, t))^{N-2}$. Just keeping the leading order terms for the diagonal and the non-diagonal terms provides the following approximation for $G_{N-1}^{(i)}$

$$G_{N-1}^{(i)} \approx (G_0(x, t))^{N-2} \left(G_0(x, t) - \sum_{j(\neq i)} G(k_i^0 - k_j^0, x, t) \right) \tag{42}$$

with an error of order $(\gamma/L)^2$. Therefore in this approximation the Pauli principle is strictly obeyed to order g^2 . To this order $\langle \hat{n}_k \rangle(t)$ in Eq.(31) can easily be calculated using $G_0 \approx 1$ and Eq.(41) in Eq.(42)

$$\begin{aligned}
\langle \hat{n}_k \rangle^{(1)}(t) \approx & \sum_i \left\{ \delta_{k, k_i^0} \left(1 - \frac{2\pi}{L} \sum_q |f_q(t)|^2 \right) + \frac{2\pi}{L} |f_{k_i^0 - k}(t)|^2 \right\} \\
& + \frac{2\pi}{L} \sum_{i,j} \left| f_{k_i^0 - k_j^0}(t) \right|^2 (\delta_{k, k_i^0} - \delta_{k, k_j^0})
\end{aligned} \tag{43}$$

where the second line on the rhs via the approximate $G_{N-1}^{(i)}$ takes care of the Pauli principle. This is most easily seen for occupancy of an initial momentum state of momentum k_l^0

$$\langle \hat{n}_{k_l^0} \rangle^{(1)}(t) \approx 1 - \frac{2\pi}{L} \sum_{q \neq (k_l^0 - k_i^0)} |f_q(t)|^2. \quad (44)$$

The electron with initial momentum k_l^0 cannot scatter into the momentum k_i^0 and none of the other electrons can scatter into momentum k_l^0 .

In the model with the coupling $g^{(1)}(q)$ gain contributions first occur in order g^4 when the phonons are in their ground state initially. For k larger than the initial momenta, i.e. $k > k_i^0, i = 1, \dots, N$ it is therefore illuminating to expand the exact solution to this order in g . One can distinguish two contributions to order g^4 . First the approximation given in Eq.(42) can be expanded to this order using Eq.(34) and Eq.(41). The correction to the result for distinguishable particles in Eq.(42) is obtained by using $(G_0(x, t))^{N-2} G(k_i^0 - k_j^0, x, t) \approx G(k_i^0 - k_j^0, x, t)$ and $F_1(x, t) \approx 1$. Only the term proportional to e^{-iqx} in the second line on the rhs of Eq.(41) contributes to the gain. The x -integration in Eq.(31) is trivial and one obtains

$$\langle n_k \rangle^{(2)}(t) = \left(\frac{2\pi}{L} \right)^2 \sum_{i < j} \left| \gamma_{k-k_i^0}(t) - \gamma_{k-k_j^0}(t) \right|^2 + O(\gamma^3). \quad (45)$$

There are two types of terms missing in Eq.(42) in order to make $G_{N-1}^{(i)}$ correct to order g^4 . They are due to single pair permutations in Eq.(32)

$$G_{N-1}^{(i), (2)} = - (G_0(x, t))^{N-3} \sum_{(m \neq n) \neq i} \left(G(k_n^0 - k_m^0, x, t) - G(k_i^0 - k_m^0, x, t) \right) G(k_m^0 - k_n^0, x, t). \quad (46)$$

Expanding this expression to order γ^2 and adding it to the approximation Eq.(42) for $G_{N-1}^{(i)}$ one obtains for k larger than the initial momenta

$$\langle n_k \rangle^{(2)}(t) = \left(\frac{2\pi}{L} \right)^2 \sum_{i < j}' \left| \gamma_{k-k_i^0}(t) - \gamma_{k-k_j^0}(t) \right|^2 + O(\gamma^3) \quad (47)$$

where the prime indicates that only the pairs (i, j) contribute to the sum for which $k_i^0 + k_j^0 - k$ is different from the other initial momenta. This result which correctly incorporates the Pauli blocking can also quite easily be derived in second order time-dependent perturbation theory for the initial state (see appendix C) and it is very helpful for the discussion of the results presented in the next figures.

In the following we present detailed numerical results for finite systems using the exact expression for $G_{N-1}^{(i)}(x, t)$ as well as the approximation presented in Eq.(42) and compare the results with the corresponding ones for distinguishable particles with the same initial momenta.

In Fig.4 the results for the distribution function of three different systems are compared at time $\omega_0 t = 50$ with the coupling $\alpha = 2\pi 10^{-3}$. In the first system there are six indistinguishable particles (fermions) initially occupying adjacent momentum states from $-5\Delta q$ to zero. In the second system the total momentum distribution for six distinguishable particles initially occupying the same states is presented. The third system corresponds to two fermions in adjacent momentum states with the same dimensionless density $N/(Lq_B)$ as the six fermion system. For initial momenta where all the particles can relax into the lower resonant momentum state by emitting a phonon with momentum q_B the difference between the fermions and the distinguishable particles is generally small in the loss part of the distribution up to intermediate times as can be seen in Fig.4. The occupation numbers in the region of the gain peak ($k = q_B$), however, differ roughly by a factor of two. For shorter times the deviations are more drastic. In appendix C the occupation numbers in the gain region are calculated in second order time-dependent perturbation theory for the initial state for fermions and distinguishable particles and the results derived there can account very well for this difference. The physical content of Eq.(C5) (agreeing with Eq.(47)) and Eq.(C6) is that a particle can be scattered into a higher momentum state with an amplitude $\gamma_q(t)$ by absorbing a phonon with momentum q which was emitted previously by a different particle. This process has an exchange process where the initial and the final state are the same but the role of the two particles as an emitter and an absorber of the phonon are exchanged. The phonons exchanged in the two processes are different but this is irrelevant for the calculation of the fermionic momentum distribution. For fermions the occupation probability for a momentum state in the gain region is the absolute square of the sum of the amplitudes for the two processes which have a relative minus sign. For distinguishable particles on the other hand the two processes can be distinguished and the probability is the

sum of the absolute square of the amplitudes for the individual processes. In Fig.4 all the initially occupied momentum states are very close and consequently all the corresponding exchange processes have a similar amplitude leading to the reduction of the weight in the gain peak for the fermions. A more detailed discussion of $\gamma_q(t)$ is given in appendix C and it shows that the shorter the time the broader are the features of the amplitude and therefore the cancellation in Eq.(47).

The interference effect contained in Eq.(47) is not properly described by the usual quantum kinetic equations [1,2] in which the collision term is treated in the Born approximation but requires an improved treatment [9].

The agreement of the two fermion system with the corresponding six particle system is very good - also for larger times. The momentum grid of the smaller system is different but the results for its momentum states nearly always agree with the results for the larger system. The approximation presented in Eq.(42) agrees with the exact solution within the plotting accuracy.

In Fig.5 the distributions of the same six particle systems as in Fig.4 are presented at time $\omega_0 t = 50$ but with the coupling strength $\alpha = 2\pi 10^{-2}$. Consequently the relaxation process is more advanced and the peaks are smoother with a larger weight in the states between them. The approximation (Eq.(42)) for the six indistinguishable particles - not shown in the figure for its clarity - gives values slightly too large for the central excitations and phonon peaks smaller than $-7q_B$ and larger than $2q_B$.

In Fig.6 the results are shown for the same systems at the same time as in Fig.5 but again with the weaker coupling $\alpha = 2\pi 10^{-3}$ and different initial momenta. Here the zero momentum state and the next two lower states are occupied and the second group of three particles has momenta shifted by $-q_B$. Therefore in the six fermion system the three particles with larger momenta cannot relax by emitting a resonant phonon. The distinguishable particles of course are not subject to this blocking and in contrast to Fig.4 one can clearly see the large difference between the two systems in the negative momentum peaks. However the difference in the first gain peak is not as large as in Fig.4. For an explanation Eq.(47)

is useful again. If one particle of the smaller and larger momentum group interact by phonon exchange the corresponding exchange process has a very different amplitude. In the one process a phonon with momentum q_B will be absorbed and in the exchange process a phonon with momentum $2q_B$. Consequently the contributions of the two processes do not cancel each other as much as in Fig.4. On the other hand processes involving two particles from the larger momentum group only do not contribute to the resonant states of the gain peak at all but the exclusion of these processes cannot compensate the other effect and the difference between the fermions and the distinguishable particles is reduced.

V. SUMMARY

We have presented the exact analytical result for the time dependence of the electronic momentum distribution for a model with a linear electronic energy dispersion for a translationally invariant initial state with N electrons and thermal phonons at temperature T_{ph} . In order to show as clearly as possible the difference between the $N = 1$ “polaron case” and the new effects occurring for $N > 1$ we have presented numerical results for $T_{ph} = 0$ only. While for distinguishable particles the influence function can be simply evaluated also for a finite *density* of particles in the thermodynamic limit, for fermions numerical results were presented only for finite particle number and system size. As shown in Fig.4 for not too large times finite systems with different N but the same *density* are very similar, which indicates that going to the thermodynamic limit is not very important. Apart from the obvious effects of Pauli-blocking interference effects play an important role which are not incorporated in quantum kinetic equations which treat the scattering term in the Born approximation [1] and [2]. As interference effects are very important to correctly describe the gain process in the short time limit our exact results can serve as an excellent testing ground for improved quantum kinetic equations.

ACKNOWLEDGMENTS

The authors would like to thank V. Meden and E. Runge for the collaboration at early stages of this work and J. Fricke and R. Zimmermann for stimulating discussions. One of us (C. W.) would like to thank the Deutsche Forschungsgemeinschaft (SFB 345 “Festkörper weit weg vom Gleichgewicht”) for financial support.

APPENDIX A:

In this appendix we present analytical results for various integrals appearing in Eqs.(22) and (23) for the model with a q -independent coupling function $g^{(2)}(q) \equiv g$ and $\omega_q \equiv \omega_0$. We first consider the integral

$$I(x, t) \equiv \int_{-\infty}^{\infty} dx \left(\frac{\sin [(\omega_0 - vq) t/2]}{(\omega_0 - vq)/2} \right)^2 e^{iqx} \quad (\text{A1})$$

which is already needed for the $N = 1$ “polaron case”. Changing the integration variable it can be written as

$$I(x, t) = \frac{2t}{v} e^{iq_B x} \int_{-\infty}^{\infty} du \frac{\sin^2(u)}{u^2} e^{-iuy} \quad (\text{A2})$$

with $y = 2x/(vt)$. Using contour integration one obtains for $t > 0$

$$I(x, t) = \frac{2\pi}{v^2} e^{iq_B x} (vt - |x|) \Theta(vt - |x|), \quad (\text{A3})$$

where $\theta(x)$ is the step function. Similarly the function

$$J(x, t) = \int_{-\infty}^{\infty} dq \frac{1}{(\omega_0 - vq)^2} \left(1 + i(\omega_0 - vq) t - e^{i(\omega_0 - vq)t} \right) e^{iqx} \quad (\text{A4})$$

which is needed in the calculation of $G_0(x, t)$ in Eq.(23) can be evaluated by contour integration, too. For $t > 0$ one has

$$J(x, t) = \frac{2\pi}{v^2} e^{iq_B x} (vt - x) \Theta(x) \Theta(vt - x). \quad (\text{A5})$$

With these results the q -integration of the functions in the integrand of the momentum distribution Eq.(36) can be performed analytically for $g^{(2)}(q)$. As a function of the dimensionless momentum variable $\tilde{k} \equiv (k - k_1^0)/q_B$ one obtains for $\tilde{n}(\tilde{k}, \tau) \equiv q_B n(k, t)$

$$\tilde{n}(\tilde{k}, \tau) = \int_{-\infty}^{\infty} \frac{du}{2\pi} e^{i\tilde{k}u} e^{\tilde{b}(u, \tau) + \tilde{n}_p \tilde{c}(u, \tau)} \quad (\text{A6})$$

where \tilde{b} and \tilde{c} for $\tau > 0$ are given by

$$\tilde{b}(u, \tau) = -\alpha\tau(1 + 2n_B(\omega_0)) + \alpha \left[e^{iu} (1 + n_B(\omega_0)) + e^{-iu} n_B(\omega_0) \right] (\tau - |u|) \Theta(\tau - |u|) \quad (\text{A7})$$

and

$$\begin{aligned} \tilde{c}(u, \tau) = & \int_{-\infty}^{\infty} dv \left[\exp \left\{ -2i\alpha[(\tau - (v - u)) \sin(v - u) \Theta(v - u) \Theta(\tau - (v - u)) \right. \right. \\ & \left. \left. - (\tau - v) \sin(v) \Theta(v) \Theta(\tau - v)] \right\} - 1 \right]. \end{aligned} \quad (\text{A8})$$

The functions obey the relations $\tilde{b}^*(u, \tau) = \tilde{b}(-u, \tau)$ and $\tilde{c}^*(u, \tau) = \tilde{c}(-u, \tau)$ which guarantee that $n(\tilde{k}, \tau)$ is real. The first term on the rhs of Eq.(A7) is equal to $\tilde{b}(\infty, \tau)$ which enters the weight $p_{k_1^0}(\tau)$ and $\tilde{c}(\infty, \tau)$ is given by

$$\tilde{c}(\infty, \tau) = 2 \int_0^\tau dv [\cos \{2\alpha(\tau - v) \sin v\} - 1] \quad (\text{A9})$$

This integral cannot be performed analytically. Expanding in powers of α yields

$$p_{k_1^0}(\tau) = \exp \left\{ -\alpha\tau(1 + 2n_B(\omega_0)) - \alpha^2 \tilde{n}_p \left(\frac{2}{3}\tau^3 - \tau + \frac{1}{2} \sin 2\tau \right) + O(g^6) \right\} \quad (\text{A10})$$

Due to the form of the functions $\tilde{b}(u, \tau)$ and $\tilde{c}(u, \tau)$ the continuous part of $n(\tilde{k}, \tau)$ can be expressed as a *finite* integral over u from zero to τ

$$\tilde{n}_{cont}(\tilde{k}, \tau) = 2\text{Re} \left(\int_0^\tau \frac{du}{2\pi} e^{i(\tilde{k} - k_1^0)u} \left[e^{\tilde{b}(u, \tau) + \tilde{n}_p \tilde{c}(u, \tau)} - p_{k_1^0}(\tau) \right] \right). \quad (\text{A11})$$

APPENDIX B:

In this appendix we shortly describe our numerical method to calculate the momentum distribution for finite systems. It is a straightforward generalization of the technique used

in [7]. As one step of the procedure can actually be simplified considerably compared to [7], we first describe the method for the simplest case $N = 1$, the coupling function $g^{(1)}(q)$ and the phonons initially in their ground state. In this case the function $F_1(x, t)$ in Eq.(21) can be expanded in a power series in $z \equiv e^{i(\frac{2\pi}{L})x}$

$$F_1(x, t) = \sum_{m=0}^{\infty} F_m(t) e^{im(\frac{2\pi}{L})x}. \quad (\text{B1})$$

Recursion relations to determine the coefficients $F_m(t)$ are discussed below. If we take $\rho^{(1)}(x) = 1/L$, i.e. the initial momentum of the particle to be $k_0 = 0$, the integration in Eq.(22) can be trivially performed and yields for $k_n = n(\frac{2\pi}{L})$

$$\begin{aligned} \langle n_{k_n}^{(1)} \rangle(t) &= \frac{1}{L} \int \sum_{m=0}^{\infty} F_m(t) e^{i(n+m)(\frac{2\pi}{L})x} dx \\ &= F_{-n}(t) \end{aligned} \quad (\text{B2})$$

for $n \leq 0$ and $\langle n_{k_n}^{(1)} \rangle(t) = 0$ for $n > 0$. In order to calculate the coefficients $F_m(t)$ we write

$$F_1(x, t) = e^{g_t(z) - g_t(1)} \equiv B e^{g_t(z)} \quad (\text{B3})$$

where the function $g_t(z)$ follows from Eq.(21) as

$$g_t(z) = \sum_{n=0}^{\infty} a_n(t) z^n \quad (\text{B4})$$

with $a_n(t) = (\frac{2\pi}{L}) |f_{n(\frac{2\pi}{L})}(t)|^2$. We now expand $e^{g_t(z)}$ in a power series in z

$$\tilde{F}_t(z) \equiv e^{g_t(z)} = \sum_{n=0}^{\infty} c_m(t) z^m. \quad (\text{B5})$$

If we use $\tilde{F}'_t(z) = g'_t(z) \tilde{F}_t(z)$ we obtain the recursion relations

$$c_m(t) = \frac{1}{m} \sum_{l=1}^m l c_{m-l} a_l(t). \quad (\text{B6})$$

Using $F_m(t) = B c_m(t)$ yields the momentum distribution for the simplest case. Already relaxing the assumption $T_{ph} = 0$ leads to a new aspect as $F_1(x, t)$ can now be written as a product of a power series in z and a power series in $1/z$. Multiplying these series and performing the integration as in Eq.(B2) leads to an expression for $\langle n_{k_n} \rangle(t)$ which involves a summation over a product of the expansion coefficients [7].

In order to calculate the momentum distribution for finite systems and $N > 1$ we also express the functions $G(n(\frac{2\pi}{L}), x, t)$ as Laurent series in z . As $G_{N-1}^{(i)}(x, t)$ is a sum over products of these functions it also can be obtained as Laurent series in z such that the final integration in Eq.(31) can be performed trivially.

APPENDIX C:

In this appendix we discuss the influence of the Pauli principle on the weight of the first gain satellite in the framework of time-dependent perturbation theory. This provides additional insight in the meaning of the result to order g^4 (Eq.(47)) which we obtained from the exact solution Eq.(31) and Eqs.(41) and (42). In order to shorten the calculation and to simplify the argument we use the coupling function $g^{(1)}(q)$ which vanishes for negative q in this appendix and assume the phonons to be initially in their groundstate $|0\rangle_{ph}$. As we assume initial statistical operators corresponding to homogeneous systems, it is sufficient to describe the time evolution of an initial state $|\mathbf{k}_0\rangle_a$ for N fermions and a product state for distinguishable particles. In the following we treat fermions and note the simplifications for distinguishable particles in the end. We calculate $\langle n_k \rangle_t$ as

$$\langle n_k \rangle(t) = \langle \phi_k(t) | \phi_k(t) \rangle \quad (C1)$$

where $|\phi_k(t)\rangle \equiv \hat{n}_k \tilde{U}(t) |\mathbf{k}_0\rangle_a |0\rangle_{ph}$ with $\tilde{U}(t)$ the time evolution operator in the interaction representation defined in Eq.(9). As we are interested in the *gain region* we assume that k is *larger* than the largest initial momentum k_{max}^0 . For the coupling function $g^{(1)}(q)$ the first order perturbation theory for $\tilde{U}(t)$ gives no contribution, i.e. the leading term is of second order in $g^{(1)}$

$$\begin{aligned} |\phi_k(t)\rangle^{(2)} &= -\hat{n}_k \int_0^t dt' \int_0^{t'} dt'' H_{ep}(t') H_{ep}(t'') |\mathbf{k}_0\rangle_a |0\rangle_{ph} \\ &= -\left(\frac{2\pi}{L}\right) \hat{n}_k \sum_{q>0} \gamma_q(t) \rho_q^\dagger \rho_q |\mathbf{k}_0\rangle_a |0\rangle_{ph}. \end{aligned} \quad (C2)$$

Here we have used Eq.(4) and the fact that the term involving $\rho_q \rho_{q'}$ does not contribute

for $k > k_{max}^0$. The function $\gamma_q(t)$ defined in Eq.(16) results from the double time integration. Using Eq.(3) or the representation of ρ_q in second quantization one obtains

$$\begin{aligned}\hat{n}_k \rho_q^\dagger \rho_q |\mathbf{k}_0\rangle_a &= \sum_{i < j} \hat{n}_k \left(\left| k_1^0, \dots, k_i^0 + q, \dots, k_j^0 - q, \dots, k_N^0 \right\rangle_a \right. \\ &\quad \left. + \left| k_1^0, \dots, k_i^0 - q, \dots, k_j^0 + q, \dots, k_N^0 \right\rangle_a \right)\end{aligned}\quad (C3)$$

where the initial momenta not written out are unshifted. Note that the states on the rhs can vanish if one (or both) of the shifted momenta coincide with the unshifted ones. This is the “trivial” manifestation of the Pauli blocking. A more subtle effect of the antisymmetry of the states occurs, if we perform the q -summation in Eq.(C2). This yields

$$\begin{aligned}|\phi_k(t)\rangle^{(2)} &= -\left(\frac{2\pi}{L}\right) \sum_{i < j} \left[\gamma_{k-k_i^0}(t) \left| k_1^0, \dots, k_i^0 + k_j^0 - k, \dots, k_N^0 \right\rangle_a \right. \\ &\quad \left. + \gamma_{k-k_j^0}(t) \left| k_1^0, \dots, k_i^0 + k_j^0 - k, \dots, k_N^0 \right\rangle_a \right]\end{aligned}\quad (C4)$$

For fermions the second term on the rhs equals the first one apart from a minus sign, while for distinguishable particles (without the subscript “a”) they are orthogonal. Using Eq.(C1) we obtain for the fermionic occupation numbers in the gain regime

$$\langle n_k \rangle^{(2)}(t) = \left(\frac{2\pi}{L}\right)^2 \sum_{i < j}' \left| \gamma_{k-k_i^0}(t) - \gamma_{k-k_j^0}(t) \right|^2 + O(\gamma^3) \quad (C5)$$

where the prime indicates that the pair (i, j) only contributes if $k_i^0 + k_j^0 - k$ is different from all the other initial momenta k_l^0 for l different from i and j . For $k - k_{max}$ larger than the range $\Delta k = k_{max} - k_{min}$ the prime on the sum can be omitted. For distinguishable particles one obtains from Eq.(C4)

$$\langle n_k \rangle_{dis}^{(2)}(t) = \left(\frac{2\pi}{L}\right)^2 \sum_{i < j} \left(\left| \gamma_{k-k_i^0}(t) \right|^2 + \left| \gamma_{k-k_j^0}(t) \right|^2 \right) \quad (C6)$$

which also follows directly from the exact solution Eq.(22) summed over all particles and the approximation for $G_0(x, t)$ presented in Eq.(34).

For a more quantitative discussion of the difference between the gain peaks from Eqs.(C5) and (C6) it is necessary to discuss the momentum dependence of $\gamma_q(t)$ for different $\tau = \omega_0 t$. The real part of $\gamma_q(t)$ which is equal to $|f_q(t)|^2$ has a peak at q_B , is symmetric to this

momentum and apart from weak oscillations falls off like $1/(q - q_B)^2$. The imaginary part of $\gamma_q(t)$ is antisymmetric with respect to q_B , with peaks near q_B and falls off like $1/(q - q_B)$. The width of the peaks in the real- and imaginary part of $\gamma_q(t)$ is inversely proportional to τ and this leads to the cancellation in Eq.(C5).

REFERENCES

- [1] R. Zimmermann, Phys. Stat. Solidi **159**, 317 (1990)
- [2] D. B. Tran Thoai and H. Haug, Phys. Rev. **B47**, 3574 (1993)
- [3] J. Schilp, T. Kuhn and G. Mahler, Phys. Rev. **B50**, 5435 (1994)
- [4] S. Haas, F. Rossi and T. Kuhn, Phys. Rev. **B53**, 12855 (1996)
- [5] V. Meden, C. Wöhler, J. Fricke and K. Schönhammer, Phys. Rev. **B52**, 5624 (1995)
- [6] D. C. Mattis and E. H. Lieb, J. Math. Phys. **6**, 304 (1965)
- [7] V. Meden, J. Fricke, C. Wöhler ,and K. Schönhammer, Z. Phys. **B 99**, 357 (1996)
- [8] for a simple proof see e.g. N. D. Mermin, J. Math. Phys. **7**, 1038 (1966)
- [9] C. Wöhler and K. Schönhammer, to be published
- [10] C. Fürst, A. Leitenstorfer, A. Laubereau, and R. Zimmermann, to be published

FIGURES

FIG. 1. Evolution of the weight of the initially occupied momentum state $p_{k_1^0}(\tau)$ in time $\tau = \omega_0 t$ with the coupling function $g^{(2)}$ and the coupling $\alpha = 2\pi 10^{-3}$. As in all the following figures the calculations were performed with phonons initially at zero temperature and the coupling $g^{(1)}$ if not indicated differently.

FIG. 2. Momentum distribution function for systems with different coupling $g^{(1)}$ and $g^{(2)}$ and different initial distributions at time $\omega_0 t = 50$. The coupling strength is always $\alpha = 2\pi 10^{-3}$ and the particle density $\tilde{n}_p = 0.001$. For the first two systems with an initially sharp momentum distribution, i.e. $\sigma = 0$ the continuous part of the distribution \tilde{n}_{cont} is shown with the weight of the initial momentum state being 0.7295 and 0.7280 for the first, and second system respectively. The difference between the two curves is only visible in the energy oscillations for positive momenta. For the third system with an initial Gaussian distribution the distribution function \tilde{n} (see (A6)) is shown.

FIG. 3. Momentum distribution function for the thermodynamic limit \tilde{n}_{cont} with different particle densities and for a finite system with 9 particles and $q_B = n_B \Delta q$ with $n_B = 40$ (Δq is the smallest momentum unit). The coupling strength is $\alpha = 2\pi 10^{-2}$. The particle density of the first two systems is the same ($\tilde{n}_p = 0.2/(2\pi)$). The weight of the initially excited state in the thermodynamic limit systems is 0.040 for the first and 0.135 for the last one. For the finite system the zero momentum component has been left out, having the value 0.042.

FIG. 4. Momentum distribution function for three finite systems with coupling strength $\alpha = 2\pi 10^{-3}$ at time $\omega_0 t = 50$. For the two systems with six fermions and six distinguishable particles we use $n_B = 42$ and for the two fermion system $n_B = 14$ in order to give the same dimensionless particle density. The occupancies of the initially occupied adjacent states at zero momentum have been rescaled by 1/5 to allow for a better resolution.

FIG. 5. The six particle systems are the same as in Fig.4 for $\omega_0 t = 50$ but with the coupling $\alpha = 2\pi 10^{-2}$.

FIG. 6. The systems and the time are the same as in Fig.5 but with $\alpha = 2\pi 10^{-3}$ and different initial momenta. Here, three adjacent momentum states at zero momentum and three shifted by $-q_B$ are initially occupied. The occupancies of these states have been again rescaled by 1/5.

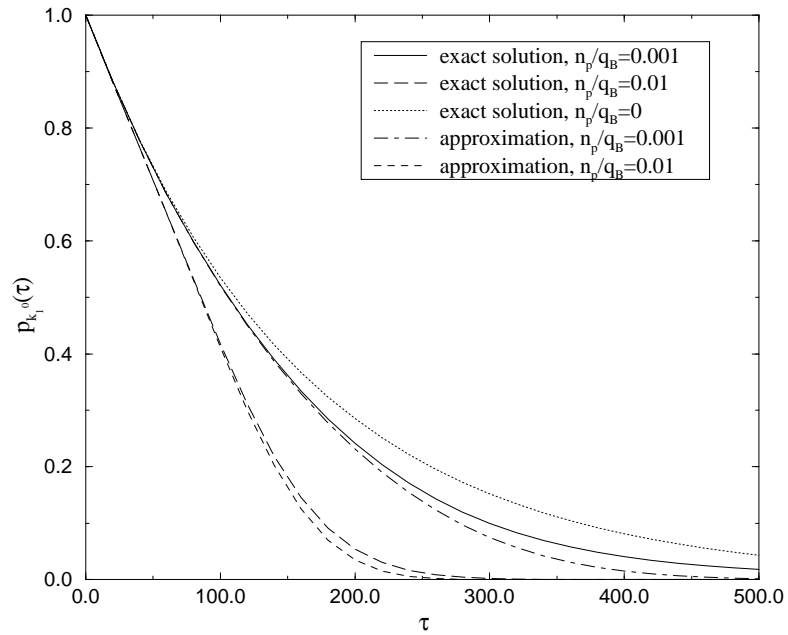


Figure 1

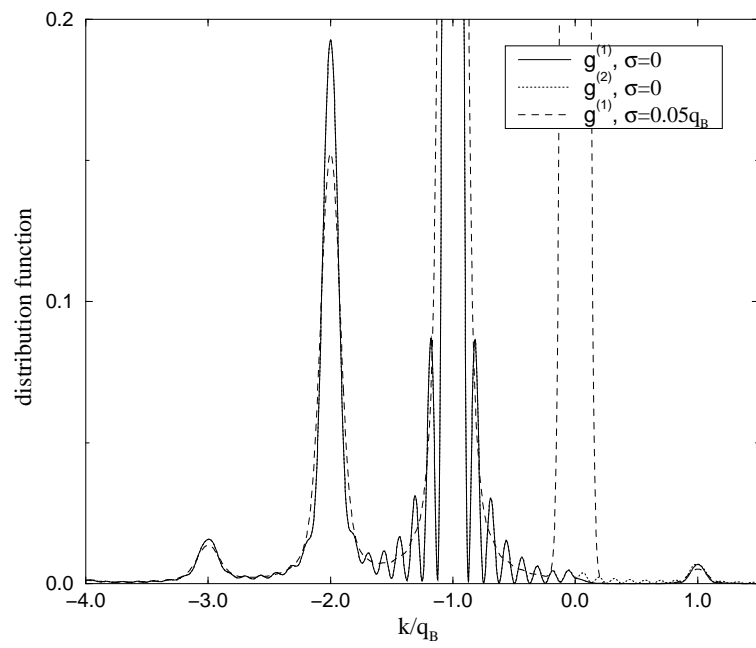


Figure 2

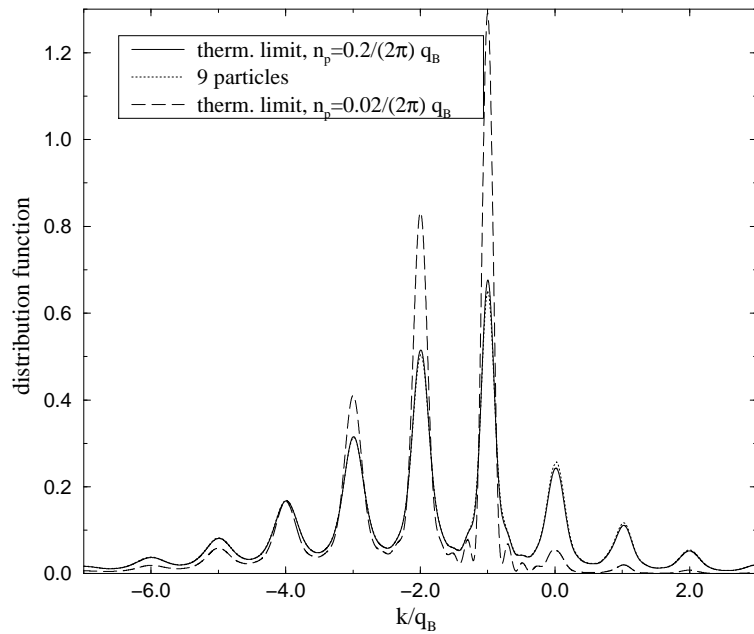


Figure 3

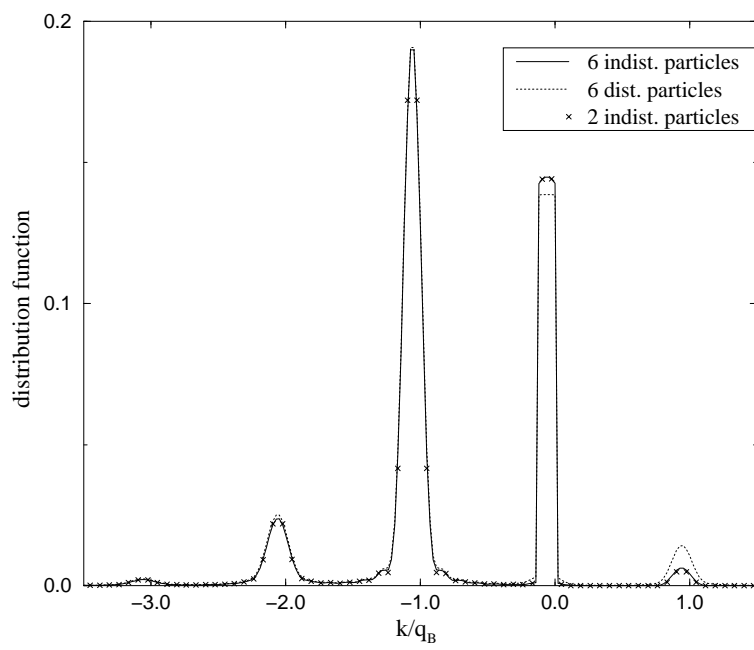


Figure 4

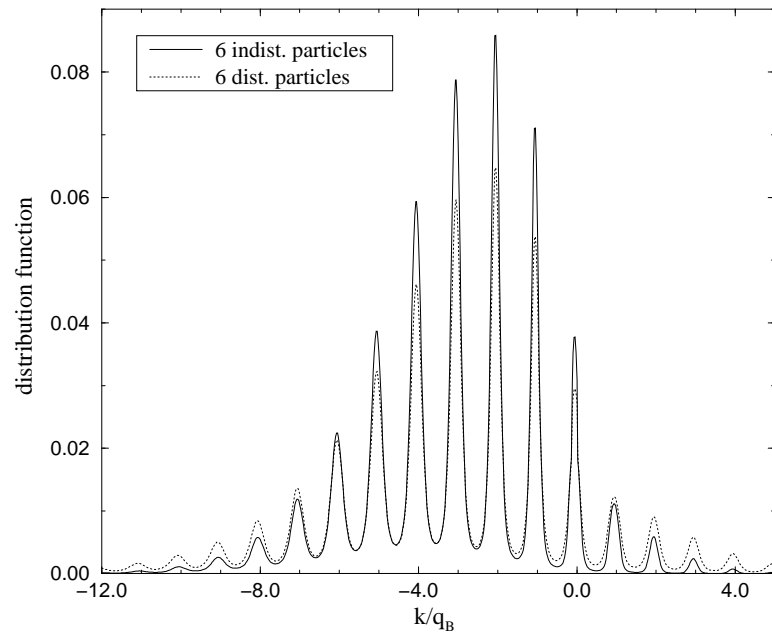


Figure 5

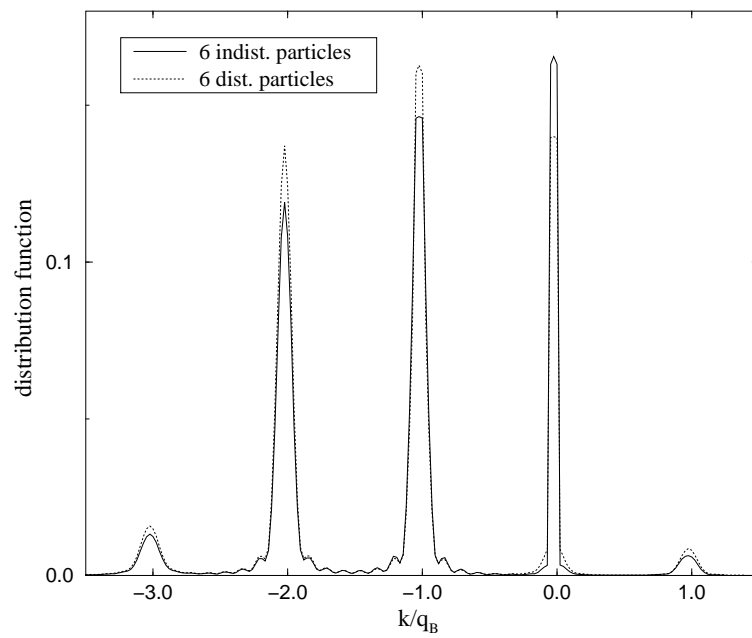


Figure 6